JCTC Journal of Chemical Theory and Computation

Donor−Acceptor Dissociation Energies of Group 13−15 Donor−Acceptor Complexes Containing Fluorinated Substituents: Approximate Lewis Acidities of $(F_3C)_3M$ vs $(F_5C_6)_3M$ and the Effects of Phosphine Steric Bulk

Austin L. Gille and Thomas M. Gilbert*

Department of Chemistry and Biochemistry, Northern Illinois University, DeKalb, Illinois 60115

Received May 24, 2008

Abstract: To study donor−acceptor complexes containing fluoroalkyl and -aryl substituents on the acceptors, ONIOM methods for optimizing large complexes and determining single point energies were tested. A two-layer ONIOM optimization procedure utilizing the MPW1K model followed by single point calculations using the composite three-layer ONIOM G2R3 method proved acceptable. The optimization model predicts M-X bond distances well when compared to experiment and shows that the distances increase discontinuously with the bulk of the phosphine. Unexpectedly, $(R_F)_3B\text{-}XR_3$ and $(R_F)_3Al\text{-}XR_3$ bond dissociation energies (ΔE_{DA}) are comparable for several R substituents. For $R_F = CF_3$, both are predicted to exhibit M-X ΔE_{DA} values in the range 55−80 kcal mol^{-1}, exceptionally strong for dative bond energies. For $R_F = C_6F_5$, the ΔE_{DA} values are predicted to lie in the range 30−45 kcal mol^{-1}. $(F_5C_6)_3BP(t\text{-}Bu)_3$, which does not contain a B−P bond, is predicted to display $\Delta E_{DA} = 19$ kcal mol^{-1}. The ΔE_{DA} energies do not change smoothly as the steric bulk of the phosphine increases. However, intrinsic ΔE_{DA} energies ΔE_{int} show a regular increase as the donor ability of the phosphine increases, confirming that the reorganization energy of the individual moieties contributes sizably to the overall ΔE_{DA}. The data indicate that PPh_3 is approximately equivalent to PMe_3 as a donor in terms of ΔE_{int}.

Introduction

Main group Lewis acid−base complexes remain of interest as archetypal tests of bonding theories but have recently gained new emphasis owing to Stephan's recent report[1] of the heterolytic cleavage of H_2 by the "frustrated Lewis pairs"[2] (FLPs) $(F_5C_6)_3BPR_3$ (R = *t*-Bu, mesityl) and $Ph_3BP(t\text{-}Bu)_3$. The steric bulk of the substituents provides the key to this reactivity, apparently by prohibiting formation of strong B−P bonds. The fluorines in the former complexes also seem to play a role, as computational studies suggest that $(F_5C_6)_3BP(t\text{-}Bu)_3$ is held together to some extent by intramolecular F...H interactions across the BP core.[3] Such effects have been observed experimentally and studied computationally for a range of $(F_5C_6)_3M\text{-}XR_3$ systems (M = B, Al; X = N, P).[4−6] It is plausible that interactions between the arene π clouds and the *t*-Bu hydrogens act similarly in $Ph_3BP(t\text{-}Bu)_3$.

Despite these extensive studies, in general the factors that determine M-X bond dissociation energies (ΔE_{DA}) in these and related fluorinated systems have not been systematically examined. Indeed, ΔE_{DA} values and trends have been examined only sparsely.[3,4] We are particularly interested in determining ΔE_{DA} values and trends for complexes where $(F_3C)_3M$ acts as the acceptor, as experiments suggest $(F_3C)_3B\text{-}NR_3$ complexes exhibit exceptionally strong B−N bonds.[7] For example, $(CF_3)_3B\text{-}NH(CH_3)_2$ forms through treatment of $[(CF_3)_3B\text{-}N(CH_3)_2]^-$ with excess concentrated HCl;[8] $(CF_3)_3B\text{-}NH(CH_2CH_3)_2$ converts to $(CF_3)_3B\text{-}NH_3$ upon treatment with excess $KOH/Br_2/H_2O$.[9] Structural and computational studies[10] show that the substituents on B and N adopt conformations intermediate between staggered and

* Corresponding author e-mail: tgilbert@niu.edu.

10.1021/ct8001859 CCC: $40.75
Published on Web 09/23/2008

Table 1. M-X Bond Distances (Å) and ΔE_{DA}(raw)[17] Values (kcal mol^{-1}) Using Different Models, Basis Sets, and ONIOM Layer Sizes (OLS)

	model	basis set	OLS	distance	ΔE_{DA}(raw)
$(F_5C_6)_3BPMe_3$	MP2	6−311++G(d,p)	1	2.046	34
	MP2	6−31+G(d)	1	2.052	31
	MPW1K	6−311++G(d,p)	1	2.022	38
	MPW1K	6−31+G(d)	1	2.026	38
	MPW1K	6311++G(d,p)	2	2.066	28
	MPW1K	631+G(d)	2	2.068	26
	MPW1K	6311++G(d,p)	3	2.069	28
	MPW1K	6311+G(d)	3	2.069	28
	MPW1K	631+G(d,p)	3	2.072	26
	MPW1K	6−31+G(d)	3	2.072	26
$(F_3C)_3AlPPh_3$	MP2	6−311++G(d,p)	1	2.401	59
	MP2	6−31+G(d)	1	2.403	59
	MPW1K	6−311++G(d,p)	1	2.380	62
	MPW1K	631+G(d)	1	2.382	63
	MPW1K	6311++G(d,p)	2	2.444	51
	MPW1K	6−311+G(d)	2	2.444	51
	MPW1K	6−31+G(d,p)	2	2.443	51
	MPW1K	6−31+G(d)	2	2.443	51
	MPW1K	6−311+G(d)	3	2.461	46
	MPW1K	6−31+G(d)	3	2.462	45

eclipsed, suggesting that intramolecular F...H interactions are less important than in the pentafluorophenyl analogues.

We published model tests on bond dissociation energies of alkyl- and fluoroalkyl borane amine complexes,[10] showing that the MP2 model gave results closest to experiment and that DFT models other than the MPW1K approach generally performed poorly. In accord with the experiments noted above, we predicted ΔE_{DA} = 68 kcal mol^{-1} for $(CF_3)_3B$-NMe_3, an exceptionally large value for a dative bond by any measure and almost four times the value for Me_3B-NMe_3. This, combined with the steric effects noted above, motivated us to examine the structures and dissociation energies for fluorinated borane acceptor−donor complexes where the donor bulk was increased systematically. From a computational chemistry standpoint, we felt that the MP2 model is too resource-intensive to apply to molecules as large as $(F_5C_6)_3BP(t\text{-}Bu)_3$, so we wanted to examine ONIOM-based approaches that would allow study of such complexes. We report here a variety of tests leading to ONIOM G2R3-based ΔE_{DA} values for the series $(R_F)_3M$-XR'_3 (R_F = F_3C, F_5C_6; M = B, Al; X = N, P; R = Me, Et, *i*-Pr, *t*-Bu, Ph). Our testing efforts suggest that the values predicted are likely to be acceptably accurate. The data provide a means of quantifying the effect of steric bulk and of the Lewis acidity of the tris(fluoroalkyl)borane moieties on these donor−acceptor systems and point to candidates for experimental study.

Computational Methods and Tests

All calculations were performed with the Gaussian 98 (G98) suite of programs.[11] As the molecules studied are far too large to study with our computational resources, we followed the approach suggested by Vreven and Morokuma for study of ΔE_{DA} of Ph_3C-CPh_3.[12] This involves the usual methodology of a composite method, such as the G_n models:[13] optimize to an acceptably accurate structure and then use this for vibrational/temperature corrections and for single point energy calculations using perturbation theory models of increasing sophistication and increasingly large basis sets. Vreven and Morokuma's contribution showed that ONIOM methods could be used to provide both an acceptable structure and the single point energies. Their three-layer ONIOM G2R approach for the single point energies, based on two-layer ONIOM B3LYP optimized structures, gave ΔE_{CC} within 1 kcal mol^{-1} of the experimental value for Ph_3C-CH_3 and suggested the quite reasonable value of ΔE_{CC} = 16 kcal mol^{-1} for Ph_3C-CPh_3.

As this method has not been broadly applied yet, and as our systems involve breaking dative bonds rather than homolytic ones, we felt it necessary to test it against datively bound systems. Testing required determining the effects of three variables. The model and basis set size affect only the optimization part of the method; the ONIOM layer space affects both the optimization and the single point calculations. Thus both structural parameters and ΔE_{DA} values were examined as test indicators. The complexes $(F_5C_6)_3B$-PMe_3 and $(F_3C)_3Al$-PPh_3 were selected for testing. These are representative of the spectrum of complexes we wished to examine because they (a) have fluorinated substituents on the acceptor moieties, (b) have the two group 13 atoms, and (c) have phenyl rings either on the donor or acceptor, which provide the most challenging part of using the ONIOM approach (see below).

The structures of the two complexes were optimized without constraints using a two level ONIOM approach, either the (MPW1K/various basis sets: MPW1K/3−21G) combination or the (MP2/various basis sets:HF/3−21G) combination (Table 1). The MP2[14] perturbation theory model was used as coded in G98, while the MPW1K model was generated using IOp keywords.[15] We selected the DFT MPW1K model, rather than the B3LYP model used by Vreven and Morokuma,[12] since we showed previously that it outperforms B3LYP significantly for both optimizations and energies of donor−acceptor complexes, particularly those where the donor and acceptor are trialkyl substituted.[10] Moreover, since the MPW1K model was designed to model transition state energies, it is plausible that it models weakly

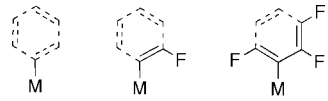

Figure 1. ONIOM layer sizes examined for phenyl/pentafluorophenyl rings. Fluorine atoms included in the high layer for pentafluorophenyl rings are shown for each layer size.

bound transition state structures well. This could prove important in modeling the structures of weakly bound donor−acceptor complexes. In many cases, the optimization procedure did not readily minimize the four parameters G98 uses to determine structural convergence. This problem has been noted previously[16] and is apparently more common when DFT methods are employed in the ONIOM approach.[12] We halted the optimization in such cases when 20 consecutive steps failed to change the predicted energy by more than 1 kcal mol^{-1}. Usually this corresponded to a point where the forces had converged but the displacements had not.

Selection of a proper layer size is a key aspect of using ONIOM. For optimizations of $(F_5C_6)_3B$-PMe_3 and $(F_3C)_3Al$-PPh_3, the Group 13/15 core atoms and the carbon atoms bound to them were always placed in the high layer; the fluorine atoms of trifluoromethyl substituents were placed there as well. Hydrogens of methyl groups were always placed in the low layer. Following Vreven and Morokuma,[12a] we examined three options for the layering of atoms of phenyl/pentafluorophenyl rings, shown in Figure 1. One can view these as the "hydrogen" level (OLS 1), the "vinyl" level (OLS 2), and the "2-butadienyl" level (OLS 3), respectively. Specifically, in OLS 1, only the core group 13/15 atoms are placed in the high level; all other atoms are added to the low level. In OLS 2, the core atoms are joined in the high layer by the phenyl ipso carbons, the phenyl ortho carbons that are oriented over the donor−acceptor axis, and the fluorines or hydrogens attached to these carbons. These selections were made so that the fluorines/hydrogens most likely to participate in intramolecular interactions (because they point toward the other half of the complex) were treated in the most extensive way available. The OLS 3 layering system works similarly save that both phenyl ortho carbons and one meta carbon, with their associated substituent atoms, are placed in the high layer. OLS 1 is the least complete but sufficiently small so that one can employ the MP2/6−311++G(d,p) model chemistry on the high level (Table 1); OLS 3 is the most complete but quite resource-intensive for C_6F_5 rings, even with the DFT model and the relatively small 6−31+G(d) basis set.

On the basis of internal consistency, the data for $(F_5C_6)_3B$-PMe_3 and $(F_3C)_3Al$-PPh_3 suggest that the OLS 1 approach performs poorly for structure and ΔE_{DA} prediction (Table 1).[17] The B−P and Al−P distances are 0.4−0.8 Å shorter, and the donor and acceptor are overbound by 8−10 kcal mol^{-1}, as compared with values predicted using more expansive layer sizes. Moreover, this approach leaves the fluorine atoms in the low layer. We felt it likely that studying intramolecular F...H interactions correctly would require having the fluorine atoms that are oriented over the donor−acceptor axis in the high layer (which holds for OLS 2 and 3). Thus, we excluded the OLS 1 model for further calculations. This necessitated excluding the ONIOM MP2:HF combination as well, as this pairing is too resource-intensive to employ at the OLS 2 level. We discarded the OLS 3 model for the opposite reason: using it provides no significant improvement either in the bond distances or ΔE_{DA} values over the OLS 2 approach.

Similarly, the data in Table 1 show that using large basis sets such as 6−311++G(d,p) or 6−311+G(d) in the high level may provide slightly more accurate structures than the smaller 6−31+G(d) basis set but does not predict significantly different ΔE_{DA} values. We therefore performed all subsequent optimizations using the ONIOM (OLS 2) (MPW1K/6−31+G(d):MPW1K/3−21G) approach. In addition to the layering choices already described, we opted to model alkyl substituents larger than methyl as methyl groups. For example, for *t*-Bu, the tertiary carbon atom only was placed in the high layer, while the primary carbons and hydrogens were placed in the low layer.

Having selected an ONIOM optimization method, we adopted Vreven and Morokuma's[12] three-layer ONIOM G2R approach (hereafter called OG2R3) for final single point energy calculations. The OG2R3 composite approximates a CCSD(T)/6−311+G(2df,2p) calculation using fifteen separate energy determinations (several of which are duplicates) to determine a final molecular energy; however, all are of sizes that are compatible with typical computational resources and require only a few hours maximum per calculation. The overall OG2R3 energy is calculated as ΔE_{DA} (OG2R3) = $\Delta E_{CCSD(T)} + \Delta E_{MP2large} - \Delta E_{MP2small}$, where $\Delta E_{CCSD(T)}$ is the energy from a three-layer ONIOM calculation symbolized as ONIOM(CCSD(T)/6−31G(d):MP2/6−31G(d):B3LYP/3−21G), $\Delta E_{MP2large}$ is the energy from a three-layer ONIOM calculation symbolized as ONIOM(MP2/6−311+G(2df,2p):MP2/6−31G(d):B3LYP/3−21G), and $\Delta E_{MP2small}$ is the energy from a three-layer ONIOM calculation symbolized as ONIOM(MP2/6−31G(d):MP2/6−31G(d):B3LYP/3−21G). For each component energy determination, the high layer was restricted, as per Vreven and Morokuma,[12a] to the two core Group 13/15 atoms. Since our resources allowed it, we chose an OLS 3 medium layer rather than Vreven and Morokuma's suggestion of OLS 2; the low layer encompassed the entire complex.

To determine the utility of the OG2R3 approach, we needed standards to compare to. As a first step, we determined the OG2R3 energies of the complexes $H_xMe_{3-x}B$-NH_xMe_{3-x} (first seven entries in Table 2), as experimental dissociation enthalpies are available for them.[10,18] It should be noted that optimizations were performed without resorting to ONIOM procedures; for the OG2R3 energies, the boron and nitrogen atoms were set in the high layer, carbon or hydrogen atoms bound to these were added to form the medium layer, and all atoms were placed in the low layer. While these simple amine-boranes do not fit our broad requirements of containing fluorinated substituents or aryl groups, they provide a sense of the agreement between experiment and theory for donor−acceptor complexes. The overall rms difference between experimental and computed energies is 2.8 kcal mol^{-1}. This value is skewed somewhat

Table 2. M-X Bond Distances (Å) and ΔE_{DA} Values (kcal mol^{-1}) for $H_xMe_{3-x}B$-NH_xMe_{3-x} and $(F_3C)_3M$-XMe_3 Complexes Using Various Approaches[a]

	model	basis set	distance	ΔE_{DA}	ΔE_{DA}(OG2R3)
H_3BNH_2Me	MPW1K	6−311++G(d,p)		33	31 (35.0)
H_3BNHMe_2	MPW1K	6−311++G(d,p)		34	33 (36.4)
H_3BNMe_3	MPW1K	6−311++G(d,p)	1.630 (1.656)	34	33 (34.8)
Me_3BNH_3	MPW1K	6−311++G(d,p)		12	16 (13.8)
Me_3BNH_2Me	MPW1K	6−311++G(d,p)		14	19 (17.6)
Me_3BNHMe_2	MPW1K	6−311++G(d,p)	1.691 (1.656)	13	19 (19.3)
Me_3BNMe_3	MPW1K	6−311++G(d,p)	1.727(1.70)	10	16 (17.6)
$(F_3C)_3BNMe_3$	MP2	6−311++G(d,p)	1.638	67	65
	MPW1K	6−311++G(d,p)	1.634	53	65
	ONIOM	6−31+G(d)	1.637	52	64
$(F_3C)_3BPMe_3$	MP2	6−311++G(d,p)	1.967	72	75
	MPW1K	6−311++G(d,p)	1.974	64	75
	ONIOM	6−31+G(d)	1.976	62	74
$(F_3C)_3AlNMe_3$	MP2	6−311++G(d,p)	2.011	57	55
	MPW1K	6−311++G(d,p)	2.003	49	55
	ONIOM	6−31+G(d)	2.007	48	55
$(F_3C)_3AlPMe_3$	MP2	6−311++G(d,p)	2.423	51	54
	MPW1K	6−311++G(d,p)	2.424	48	54
	ONIOM	6−31+G(d)	2.423	48	54

[a] ΔE_{DA} values in the left most column are those from the model chemistry listed, and ΔE_{DA}(OG2R3) entries are single point ONIOM G2R3 values using the optimized structures from the listed model chemistries. Experimental values are in parentheses.

by the large differences seen for the H_3B-NR_3 complexes; the rms error for the four Me_3B-NR_3 complexes is only 1.6 kcal mol^{-1}. The data set is too small to allow firm conclusions to be drawn, but it appears that the OG2R3 approach gives ΔE_{DA} values that should differ no more than 5 kcal mol^{-1} from experiment on average.

While no experimental ΔE_{DA} values for $(R_F)_3M$-XMe_3 complexes exist, we showed previously that the MP2/6−311++G(d,p) method gives results most in agreement with experiment for $H_xMe_{3-x}B$-NH_xMe_{3-x} complexes.[10] As a second step, we selected the four $(F_3C)_3M$-XMe_3 molecules as standards, since they are small enough to allow use of this model. As these do not contain phenyl rings, setting the ONIOM layers was straightforward. For the optimizations, the high layer contained the Group 13/15 core atoms and the carbons, while the low layer encompassed the entire complex. For the OG2R3 energy calculations, the high layer included only the core Group 13/15 atoms, the medium layer added the carbons to these, and the low layer held the entire complex. Data appear in Table 2. The OLS 2 ONIOM MPW1K distances for the complexes agree well with the standard MP2 and MPW1K distances, indicating that this model performs adequately for structure prediction. The ONIOM MPW1K approach, like the full MPW1K model, systematically underbinds the complexes, slightly for the Al systems and significantly for the B systems. However, the OG2R3 composite performs superbly, in that it predicts essentially identical energies regardless of the model employed and that it agrees very well with the MP2/6−311++G(d,p) standard values at a fraction of the resource cost.

Combining these results, we thus chose to perform all further production calculations using ONIOM MPW1K/6−31+G(d):MPW1K/3−21G optimizations with the high layer containing OLS 2 atoms for phenyl/pentafluorophenyl substituents, donor/acceptor-bound carbons for methyl/trifluoromethyl substituents, and trifluoromethyl group fluorine atoms. All other atoms were placed in the low layer. Optimized structures were used as bases for OG2R3 single point energy calculations with the two core Group 13/15 atoms in the high layer, a medium layer employing OLS 3 for aryl rings, carbon atoms for alkyl groups and fluorine atoms for CF_3 substituents, and a low layer covering the entire complex.

To obtain zero point energies (ZPEs), the structures found using ONIOM optimizations were used as starting points for optimizations using the Hartree−Fock/3−21G approach. Structures were proved to be minima by analytical frequency analysis at this level. ZPEs obtained were scaled by 0.9207 when used to correct the raw energy values,[19a] giving the final values listed in Table 4. In a few instances ($(F_5C_6)_3BP(i\text{-}Pr)_3$, for example), we found that the ONIOM-predicted structure differed significantly from that predicted by HF/3−21G, in that the M-X bond was significantly longer with the smaller basis set. This almost certainly reflects the absence of diffuse and polarization functions in the 3−21G basis set. We therefore redetermined the ZPEs for these and their components using frequency calculations employing the two-layer ONIOM approach. ZPEs obtained this way were not scaled when used to correct the raw energies. ΔE_{DA} values calculated this way differed insignificantly from those calculated using HF/3−21G ZPEs.

In the Discussion section below, we will refer to intrinsic bond dissociation energy, ΔE_{int}. This term arises from broader methods of bond energy decomposition; it is sometimes called the snap bond energy or the instantaneous interaction energy.[20] The characterization and use of ΔE_{int} has been discussed in several places, so we describe it only briefly.

One way ΔE_{DA} may be decomposed is as follows

$$\Delta E_{DA} = \Delta E_{int} - \Delta E_{prep} = \Delta E_{int} - (\Delta E_{prep}(D) + \Delta E_{prep}(A))$$

where the reorganization energy ΔE_{prep} is the energy associated with deforming/relaxing the fragments of interest to their geometries in the molecule/ion (equally, the difference between the energy of the free moiety and that of the energy

Table 3. Selected Structural Parameters for Donor−Acceptor Complexes (Distances in Å, Angles in deg) at the ONIOM MPW1K/6-31+G(d):MPW1K/3-21G Level

	M-X	C-M-X-C	no. of F...H < 2.6	no of F...H/max no. of F...H
$(F_3C)_3BNMe_3$	1.637	41.3	9	
$(F_3C)_3BPMe_3$	1.976	40.2	0	0
$(F_3C)_3BPEt_3$	1.987	51.4	6	0.5
$(F_3C)_3BP(i\text{-}Pr)_3$	2.048	59.5	9	0.38
$(F_3C)_3BP(t\text{-}Bu)_3$	2.163	46.2	9	0.38
$(F_3C)_3BPPh_3$	2.016	29.6	3	1
$(F_3C)_3AlNMe_3$	2.007	45.2	2	
$(F_3C)_3AlPMe_3$	2.423	44.7	0	0
$(F_3C)_3AlPEt_3$	2.421	51.8	0	0
$(F_3C)_3AlP(i\text{-}Pr)_3$	2.437	50.9	6	0.25
$(F_3C)_3AlP(t\text{-}Bu)_3$	2.442	38.9	8	0.33
$(F_3C)_3AlPPh_3$	2.443	40.2	3	1
$(F_5C_6)_3BNMe_3$	1.797	16.4		
$(F_5C_6)_3BPMe_3$	2.068	14.9		
$(F_5C_6)_3BPEt_3$	2.077	16.4		
$(F_5C_6)_3BP(i\text{-}Pr)_3$	2.194	0.4		
$(F_5C_6)_3BP(t\text{-}Bu)_3$	3.838	5.4		
$(F_5C_6)_3BPPh_3$	2.159	0.3		
$(F_5C_6)_3AlNMe_3$	2.060	22.0		
$(F_5C_6)_3AlPMe_3$	2.454	20.6		
$(F_5C_6)_3AlPEt_3$	2.438	21.4		
$(F_5C_6)_3AlP(i\text{-}Pr)_3$	2.519	26.4		
$(F_5C_6)_3AlP(t\text{-}Bu)_3$	2.621	15.7		
$(F_5C_6)_3AlPPh_3$	2.503	5.4		

Table 4. ΔE_{DA}, ΔE_{DA}(raw),[17] ΔE_{prep}, and ΔE_{int} Energies (kcal mol^{-1}, OG2R3 Model) for Donor−Acceptor Complexes

	ΔE_{DA}	ΔE_{DA}(raw)	ΔE_{prep}(A)	ΔE_{prep}(D)	ΔE_{int}[a]
$(F_3C)_3BNMe_3$	64	71	25	3	99
$(F_3C)_3BPMe_3$	74	77	20	6	103
$(F_3C)_3BPEt_3$	70	73	21	13	107
$(F_3C)_3BP(i\text{-}Pr)_3$	77	81	29	8	118
$(F_3C)_3BP(t\text{-}Bu)_3$	69	74	40	6	120
$(F_3C)_3BPPh_3$	68	71	22	5	98
$(F_5C_6)_3BNMe_3$	21	25	29	5	59
$(F_5C_6)_3BPMe_3$	41	44	20	4	68
$(F_5C_6)_3BPEt_3$	36	39	22	11	72
$(F_5C_6)_3BP(i\text{-}Pr)_3$	32	33	29	6	68
$(F_5C_6)_3BP(t\text{-}Bu)_3$	19	20	1	0	21
$(F_5C_6)_3BPPh_3$	39	41	20	3	64
$(F_3C)_3AlNMe_3$	55	59	7	1	67
$(F_3C)_3AlPMe_3$	54	56	6	5	67
$(F_3C)_3AlPEt_3$	51	53	7	12	72
$(F_3C)_3AlP(i\text{-}Pr)_3$	68	71	10	6	87
$(F_3C)_3AlP(t\text{-}Bu)_3$	79	82	15	5	102
$(F_3C)_3AlPPh_3$	52	54	8	4	66
$(F_5C_6)_3AlNMe_3$	39	42	10	2	55
$(F_5C_6)_3AlPMe_3$	43	44	7	4	55
$(F_5C_6)_3AlPEt_3$	39	41	8	11	60
$(F_5C_6)_3AlP(i\text{-}Pr)_3$	42	44	15	9	68
$(F_5C_6)_3AlP(t\text{-}Bu)_3$	42	46	20	3	69
$(F_5C_6)_3AlPPh_3$	44	46	8	3	57
$Ph_3BP(t\text{-}Bu)_3$	5	5	0	0	5
Ph_3BPPh_3	22	22	20	2	44

[a] See the Computational Methods section.

of the moiety fixed in the orientation it has when bound to another moiety), and ΔE_{int} is therefore the intrinsic energy of the bond; that is, the energy required to dissociate the moieties from each other before they relax to their preferred separated structures. ΔE_{prep} here is treated as a positive value. It may be further subdivided into ΔE_{prep}(D), the energy associated with deforming/relaxing the donor moiety, and ΔE_{prep}(A), the analogous energy for the acceptor moiety.

This equation can be rewritten to define ΔE_{int}:

$$\Delta E_{int} = \Delta E_{DA} + (\Delta E_{prep}(D) + \Delta E_{prep}(A))$$

This equation is that used to calculate ΔE_{int} values in Table 4. One should be aware that, as ΔE_{prep}(D) and ΔE_{prep}(A) correspond to energies of species not necessarily at their structural minima, they cannot be properly corrected for ZPE, as the mathematics of ZPE estimation require use of a minimum structure. Therefore, when determining ΔE_{int}, one must use ΔE_{DA} uncorrected for ZPE. In Table 4 and the associated discussion, these uncorrected ΔE_{DA} values will be referred to as raw ΔE_{DA} values and symbolized as ΔE_{DA}(raw).[17]

Though we will not examine this here, it may be of interest to know that ΔE_{int} may be considered composed of three terms: ΔE_{elstat}, the electrostatic interaction energy between the fragments; $\Delta E_{orbital}$, the energy associated with relaxation of the orbitals as self-consistency is reached; and ΔE_{Pauli}, the repulsive interaction energy between the fragments resulting from interactions between occupied orbitals. ΔE_{elstat} and $\Delta E_{orbital}$ broadly describe electrostatic and covalent attractive aspects of bonding, respectively, while ΔE_{Pauli} describes repulsive aspects.

As the OG2R3 composite employs relatively small basis sets for many of the energy determinations, it is useful to examine the basis set superposition energy (BSSE) corrections for systems like those here. However, few examples of BSSE-corrected ONIOM calculations have appeared.[21] This stems largely from two issues: one, the Gaussian program does not allow keyword-based calculation of BSSE for ONIOM runs (the Counterpoise[22] and ONIOM keywords cannot be used in the same run); and two, each BSSE run requires five separate energy determinations, thus being resource-intensive. For our OG2R3 energies, determining the BSSE for a particular molecule requires determining indi-

vidual BSSEs using six different model chemistry/layer combinations: CCSD(T)/6−31G(d) (the BSSE of which is hereafter denoted A), MP2/6−311+G(2df,2p) (B), and MP2/6−31G(d) (C) BSSEs for the small layer; MP2/6−31G(d) (D) and B3LYP/3−21G (E) BSSEs for the medium layer; and the B3LYP/3−21G (F) BSSE for the low layer. Thus a total of 30 individual energy calculations must be performed per molecule to estimate the BSSE by the counterpoise method. This is too demanding to be practical; thus we selected two molecules, $(F_3C)_3BPPh_3$ and $(F_5C_6)_3AlPMe_3$, and determined the BSSE of each on the assumption that the values would be representative. The relevant equation combining the individual BSSEs to give a total BSSE is as follows: BSSE (total) = (A + B − C) + (D − C) − (E − F).

The values are 18.2 and 10.6 kcal mol^{-1}, respectively, so on average one expects BSSEs for molecules in the set to be 14−15 kcal mol^{-1}.

These BSSEs appear large compared to those typical and call into question the utility of the OG2R3 approach. We examined the BSSEs of each model chemistry/layer combination, finding that those for the small layers (the A + B − C part) combined contributed only 2−3 kcal mol^{-1} to the total, while the B3LYP model chemistry part (E−F) contributed less than 1 kcal mol^{-1}. The largest contribution to overall BSSE comes from the MP2-based (D−C) part, wherein the BSSE of the MP2/6−31G(d)/medium layer component is much larger than the BSSE of the MP2/6−31G(d)/small layer component. This suggests that using a smaller layer size for the former will lower the (D−C) correction and so the overall BSSE. We plan to explore this in future work. For now, we note that the BSSEs represent upper limits to the correction, and so the real correction for a particular molecule may be lower. In particular, the average BSSE probably cannot be applied to the weakly bound $(F_5C_6)_3BP(t\text{-}Bu)_3$ and $Ph_3BP(t\text{-}Bu)_3$ complexes, as these cannot readily share basis functions owing to the long distances between donor and acceptor atoms.

Results and Discussion

Structures. The predicted structures (Table 3) of these donor−acceptor complexes display no remarkable features save those noted below. As mentioned, $(F_5C_6)_3M\text{-}XR_3$ complexes have previously been analyzed computationally and experimentally in terms of the impact of intramolecular forces on structure, particularly the observation of F...H interactions and eclipsed (or nearly so) conformations. We refer the reader to that work[3−6] and simply note here several observations. First, our optimization method appears to give excellent agreement with experiment. For example, the B−P distance in $(F_5C_6)_3B\text{-}PMe_3$ is 2.061(4) Å;[23] we predict 2.068 Å. The B−P distance in $(F_5C_6)_3B\text{-}PPh_3$ is 2.180(6) Å;[5] we predict 2.158 Å, an improvement over the DFT-D-PBE/TZVP level prediction of 2.22 Å.[6] With this in mind, we note the method predicts a B−P distance of 3.838 Å for $(F_5C_6)_3BP(t\text{-}Bu)_3$, some 0.4 Å shorter than that predicted by Pàpai et al.[3] Second, the M-P bond distances in the $(F_5C_6)_3B\text{-}PR_3$ series are nearly identical for R = Me and Et, increase about 0.1 Å for R = *i*-Pr and Ph, and then increase again for R = *t*-Bu (substantially for M = B). This suggests similar steric bulk for *i*-Pr and Ph substituents, somewhat at odds with their suggested cone angles.[24] However, the view is supported by the similar M-P distances for the $(F_5C_6)_3M\text{-}P(i\text{-}Pr)_3$ and $(F_5C_6)_3M\text{-}PPh_3$ complexes, which are quite distinct from, for example, the M-P distances in $(F_5C_6)_3M\text{-}PEt_3$ or $(F_5C_6)_3MP(t\text{-}Bu)_3$. Third, the method finds six intramolecular F...H interactions of ≤2.6 Å (the sum of the van der Waals radii) for $(F_5C_6)_3B\text{-}PR_3$ (R = Me, Et, *i*-Pr) but only three for R = *t*-Bu and Ph. In the case of R = *t*-Bu, this reflects the long B−P distance; in the case of R = Ph, it reflects the planarity of the phenyl substituents. Analogous results are seen for the aluminum complexes. This illustrates the point that the core bond distance, the substituent geometry, and the number of hydrogens available all determine the number of intramolecular contacts, and thus one must analyze the data carefully to ascertain the presence and importance of such contacts. Fourth, in support of this view, the torsional angles rapidly *decrease* with the steric bulk of the phosphorus-bound substituents; i.e. as the substituents get larger, the complexes adopt more eclipsed geometries, in stark contrast to expectation. This effect is most pronounced for the borane-phosphines (some ambiguity exists on this point for the borane systems owing to the lack of a B−P bond in $(F_5C_6)_3BP(t\text{-}Bu)_3$) but appears in the alane-phosphines as well. It is notable that PPh_3 complexes show the most eclipsed conformations; this may reflect the presence of π-π interactions arising from intramolecular ring stacking in addition to the F...H interactions.[6]

No detailed analyses of intramolecular interactions in $(F_3C)_3M\text{-}XR_3$ complexes have appeared. We commented on the structures of $(F_3C)_3B\text{-}NR_3$ (R = H, Me) complexes previously, comparing computational to experimental results.[10] At that time, the observation of conformational deviations from staggered structures was of minor concern, being reflected mostly in the energies required to rotate groups around the B−N bonds. It is appropriate here to expand on this, including different core atoms and larger substituents. Before doing so, we note that the $(F_3C)_3M$ complexes display M-X bond distances markedly shorter than those for $(F_5C_6)_3M$ complexes (Table 2). This is particularly true for the $(R_F)_3M\text{-}NMe_3$ systems, where the differences are 0.16 Å for B and 0.053 Å for Al. The extent to which the distances increase in $(F_3C)_3M\text{-}PR_3$ complexes as the phosphine bulk increases from R = Me to R = *i*-Pr is smaller as well. Both observations suggest that the CF_3 substituent is more electron-withdrawing and sterically smaller than the C_6F_5 group.[25]

The data in Table 3 point out the difficulties in assessing the importance of intramolecular F...H interactions for $(F_3C)_3M\text{-}XR_3$ complexes but in general suggest that they are of little importance. First, the $F_3C\text{-}B\text{-}P\text{-}C$ torsion angles are much closer to the ideal staggered value of 60° than are their $F_5C_6\text{-}B\text{-}P\text{-}C$ counterparts. Also, the torsion angles do not vary regularly with the size or number of H atoms available for intermolecular interactions. One sees that for M = B and Al, the angle increases with the size of the R substituent to a maximum for R = *i*-Pr (i.e., the conformation becomes more staggered as size increases) and then decreases for R

= *t*-Bu. This holds for M = Al despite the fact that the Al−P bond distance increases relatively little across the series. Moreover, while the number of F...H distances ≤2.6 Å increases with the size and number of hydrogen atoms, the ratio of these to the maximum number of possible such interactions remains fairly constant.[26]

Considering all these observations, it is clear that the structural data do not allow an unambiguous evaluation of the presence or importance of intramolecular interactions here, but they are clearly less important than in the pentafluorophenyl systems. The close contacts observed may simply reflect the steric needs of the substituents compared to the sizes of the core atoms. One notes in this regard that $(F_3C)_3B$-NMe_3 and $(F_3C)_3B$-PEt_3 exhibit respectively nine and six F...H distances ≤2.6 Å, while the Al analogues exhibit none. The torsional angles clearly express competition between the steric needs of the substituents vs attempts to create close F...H contacts. As will be seen below, the energetic data provide a clearer means by which to assess the importance of intramolecular interactions and support their minimal contribution to the ΔE_{DA} values.

Donor−Acceptor Dissociation Energies. The ΔE_{DA} (OG2R3) values for the $(R_F)_3M$-XR_3 complexes studied appear in the first column of Table 4. As $(F_5C_6)_3BP(t\text{-Bu})_3$ uniquely does not contain a B−P bond, we except it from the discussion save when we include it explicitly. That said, several observations can be made, and several trends discerned.

The $(F_3C)_3BXR_3$ complexes display slightly larger ΔE_{DA} values than do their Al analogues, but the $(F_5C_6)_3BXR_3$ complexes display slightly smaller ΔE_{DA} values than their Al analogues. This presumably reflects crowding of the more compact boron systems with the larger fluoroaryl substituents. This finds support in the observation that ΔE_{DA} values for the $(F_5C_6)_3AlPR_3$ systems scarcely change as the phosphine increases in size, while those for the boron analogues decrease regularly, culminating in the lack of a B−P interaction in $(F_5C_6)_3BP(t\text{-Bu})_3$ (although this still shows a sizable dissociation energy of 19 kcal mol^{-1}).

As defined by relative ΔE_{DA} values, the $(F_3C)_3B$ moiety is a much stronger Lewis acid than is the $(F_5C_6)_3B$ moiety. Timoshkin and Frenking[27] have recently calculated ΔE_{DA} values for (aryl)- and (fluoroaryl)boranes, alanes, and gallanes, finding that all three Group 13 $M(C_6F_5)_3$ species are essentially as Lewis acidic as the corresponding MCl_3 species. They describe $Al(C_6F_5)_3$ as "one of the strongest Lewis acids". The data in Table 4 clearly show that $B(CF_3)_3$ is approximately twice as strong as this as assessed by ΔE_{DA}, while $Al(CF_3)_3$, if prepared, would be about 1.3 times as strong. These views are supported by the unusual stability of $(F_3C)_3B$ complexes noted above (and by its nonexistence as a free borane). The synthesis of $Al(CF_3)_3$ and further studies of the reactivities of both $M(CF_3)_3$ would be of considerable interest; that said, the bonds between these and donors may prove too strong to break easily, limiting their chemistry.

As mentioned above, the structural data provide little support for the presence of intramolecular F...H interactions in $(F_3C)_3MXR_3$ complexes. The energetic data show similar lacks. The ΔE_{DA} values for the systems showing the most extensive close F...H contacts, the $(F_3C)_3BPR_3$ series, change little as the number of phosphine H atoms increases. One would anticipate that, if such interactions were important, ΔE_{DA} for $(F_3C)_3BP(t\text{-Bu})_3$, with 9 F...H contacts ≤2.6 Å, would be sizably larger than that for $(F_3C)_3BPMe_3$, with no such short contacts. This does not hold. It is true that ΔE_{DA} values for the $(F_3C)_3AlPR_3$ series increase with size, so possibly intramolecular contacts play a larger role for these. We cannot assess this quantitatively given the data in hand.

In contrast to the general view that bonds between elements higher in the Periodic Table exhibit larger dissociation energies, the M-P bonds are generally stronger than the M-N bonds. Surprisingly, this holds particularly for B-N/B-P systems, where 2p-2p orbital overlap in the former is usually thought to provide stronger bonding than 2p-3p overlap in the latter. Jacobsen et al. analyzed[4] the related $(F_5C_6)_3B$-NCMe and $(F_5C_6)_3B$-PH_3 complexes, finding that the smaller covalent and electrostatic bonding interactions in the borane-phosphine were countered significantly by decreased electronic repulsions resulting from the longer B-P bond length. It appears similar effects occur here.

We noted above that, in terms of the M-P bond length, PPh_3 appeared similar to $P(i\text{-Pr})_3$. In terms of ΔE_{DA} values, PPh_3 is clearly most similar to PMe_3. This holds particularly when considering intrinsic ΔE_{int} energies, indicating that the electronic properties of the two are similar. Since PPh_3 is generally observed to be a poorer donor than PMe_3, this suggests that the interplay between bonding attractions and electronic repulsions mentioned above applies here as well. In every case, the $(R_F)_3M$-PPh_3 bond is longer than the $(R_F)_3M$-PMe_3 bond, so the repulsions decrease in the former apparently to the same extent that the attractions increase in the latter.

Curiously, the dissociation energies for $(R_F)_3M$-PR_3 complexes change erratically with the size of the phosphine. This holds despite the fact that the M-P bonds increase in length fairly regularly as the phosphine bulk increases along the series. This suggests a fairly flat potential energy surface for bond breaking in these systems. It also suggests that the reorganization energy ΔE_{prep} of the fragments contributes detectably to the overall ΔE_{DA}.

The data in Table 4 bear this out. One sees that, as expected, generally ΔE_{prep} is substantially larger for the acceptors than for the donors, as the acceptors change geometry from pseudotetrahedral to pseudotrigonal planar, while the donors change only from pseudotetrahedral to pseudopyramidal. ΔE_{prep} is larger for boranes than for alanes, because the more compact boranes encounter more repulsions as the substituents adjust from being 120° apart to being at more acute angles. Interestingly, the ΔE_{prep} values for the acceptors are approximately the same for $(F_3C)_3M$ and $(F_5C_6)_3M$ complexes for a particular M, indicating that the parameter is fairly insensitive to the size or electron-withdrawing properties of the fluorinated substituents. The total $\Delta E_{prep} = (\Delta E_{prep}(A) + \Delta E_{prep}(D))$ tends to increase from $(R_F)_3MPMe_3$ to $(R_F)_3MP(t\text{-Bu})_3$; this value for PPh_3 complexes tends to mimic that for PMe_3 complexes (see above). Of course, $(F_5C_6)_3BP(t\text{-Bu})_3$, which represents a "bound"

system where the fragments are already in their relaxed forms, shows $\Delta E_{prep} \approx 0$.

The intrinsic dissociation energies ΔE_{int} increase regularly with the size of the phosphine, indicating that they represent only the effect of increasing phosphine basicity. Remarkably, the model predicts $(F_3C)_3BP(t\text{-}Bu)_3$ to display $\Delta E_{int} = 120$ kcal mol^{-1}, a value in excess of most covalent bonds spilt homolytically. ΔE_{int} values for PPh_3 complexes are closest to those for PMe_3 complexes, reiterating the view that these two donors behave similarly. It is evident that all these $(R_F)_3MXR_3$ complexes are strongly bound, making Stephan's discovery of the distinctiveness of weakly bound $(F_5C_6)_3BP(t\text{-}Bu)_3$ all the more impressive. That this complex is so reactive despite its being bound by 20 kcal mol^{-1} indicates that this value represents an approximate "reactivity limit"; complexes with dissociation energies much larger than this are likely to be unreactive.

We have included in Table 4 our calculated dissociation energies for $Ph_3BP(t\text{-}Bu)_3$ and Ph_3BPPh_3. The former, as noted in the Introduction, also heterolytically breaks the H_2 bond; we included the latter for comparison as a phosphine-borane with large substituents. The complexes differ in that we find the *t*-Bu complex to be weakly bound by dispersion effects and not to contain a B−P bond, while the latter contains a B−P bond but displays a dissociation energy similar to that of $(F_5C_6)_3BP(t\text{-}Bu)_3$. The data show that $Ph_3BP(t\text{-}Bu)_3$ is bound by only 5 kcal mol^{-1}. This implies that F...H interactions in the fluorinated homologue $(F_5C_6)_3BP(t\text{-}Bu)_3$ contribute ca. 15 kcal mol^{-1} to the binding energy. The weak dissociation energy implies that if separation of the fragments dictates the H_2 splitting rate, then the parent system should react faster. In fact, it reacts more slowly,[1] implying that another factor, such as the Lewis acidity of the acceptor, is critically important in determining the rate. This being so, it seems plausible that the H_2 splitting involves the "reaction cell" mechanism suggested by Papai et al.[3a] See the Computational Methods section.

Conclusions

The OG2R3 model predicts dissociation energies of large donor−acceptor complexes with acceptable resource usage. As a reviewer noted, it is impossible to tell whether the energies are trustworthy, as no comparable experimental data exist. That said, they agree reasonably with known experimental energies and are consistent with the reactivity patterns exhibited by systems for which dissociation energies are unknown. We hope that such large complexes can be examined this way will spur effort to examine systems that previously were simplified.

From an experimental standpoint, the data suggest that one should be able to isolate all the $(R_F)_3MXR_3$ complexes examined. Difficulties in this regard lie in the systems finding other reaction pathways,[28] but assiduous effort should overcome this. While $(F_5C_6)_3BP(t\text{-}Bu)_3$ has so far defied isolation, the interaction energy is large enough that one could conceivably crystallize it, but the fact that it is bound through dispersive effects means that no spectroscopic method is likely to detect it. Only $Ph_3BP(t\text{-}Bu)_3$ appears to have too little binding energy to allow its isolation, and so far the reactivity of this complex does not merit extensive study.

Our finding that PPh_3 mimics PMe_3 in terms of the M-P bond length and dissociation energy is intriguing, given that the proton affinities of the two are so different. We plan to probe the reasons for this observation, beginning with the hypothesis that, for a sufficiently sized acceptor, the steric and electronic effects associated with binding cancel.

Acknowledgment. The NIU Computational Chemistry Laboratory was created using funds from the U.S. Department of Education Grant P116Z020095 and is supported in part by the taxpayers of the State of Illinois.

Supporting Information Available: Optimized Cartesian coordinates of all molecules examined, with absolute energies. This material is available free of charge via the Internet at http://pubs.acs.org.

References

(1) Welch, G. C.; Stephan, D. W. *J. Am. Chem. Soc.* **2007**, *129*, 1880–1881.

(2) Stephan, D. W. *Org. Biomol. Chem.* **2008**, *6*, 1535–1539.

(3) (a) Rokob, T. A.; Hamza, A.; Stirling, A.; Soós, T.; Pápai, I. *Angew Chem. Int. Ed.* **2008**, *47*, 2435–2438.

(4) Jacobsen, H.; Berke, H.; Dšring, S.; Kehr, G.; Erker, G.; Fröhlich, R.; Meyer, O. *Organometallics* **1999**, *18*, 1724–1735.

(5) Mountford, A. J.; Lancaster, S. J.; Coles, S. J.; Horton, P. N.; Hughes, D. L.; Hursthouse, M. B.; Light, M. E. *Inorg. Chem.* **2005**, *44*, 5921–5933.

(6) Spies, P.; Fröhlich, R.; Kehr, G.; Erker, G.; Grimme, S. *Chem. Eur. J.* **2008**, *14*, 333–343.

(7) Pawelke, G.; Bürger, H. *Appl. Organomet. Chem.* **1996**, *10*, 47–174.

(8) Brauer, D. J.; Bürger, H.; Dörrenbach, F.; Krumm, B.; Pawelke, G.; Weuter, W. *J. Organomet. Chem.* **1990**, *385*, 161–172.

(9) Pawelke, G. *J. Fluorine Chem.* **1995**, *73*, 51–55.

(10) Gilbert, T. M. *J. Phys. Chem. A* **2004**, *108*, 2550–2554.

(11) Frisch, M. J.; Trucks, G. W.; Schlegel, H. B.; Scuseria, G. E.; Robb, M. A.; Cheeseman, J. R.; Zakrzewski, V. G.; Montgomery, J. A., Jr.; Stratmann, R. E.; Burant, J. C.; Dapprich, S.; Millam, J. M.; Daniels, A. D.; Kudin, K. N.; Strain, M. C.; Farkas, O.; Tomasi, J.; Barone, V.; Cossi, M.; Cammi, R.; Mennucci, B.; Pomelli, C.; Adamo, C.; Clifford, S.; Ochterski, J.; Petersson, G. A.; Ayala, P. Y.; Cui, Q.; Morokuma, K.; Rega, N.; Salvador, P.; Dannenberg, J. J.; Malick, D. K.; Rabuck, A. D.; Raghavachari, K.; Foresman, J. B.; Cioslowski, J.; Ortiz, J. V.; Baboul, A. G.; Stefanov, B. B.; Liu, G.; Liashenko, A.; Piskorz, P.; Komaromi, I.; Gomperts, R.; Martin, R. L.; Fox, D. J.; Keith, T.; Al-Laham, M. A.; Peng, C. Y.; Nanayakkara, A.; Challacombe, M.; Gill, P. M. W.; Johnson, B.; Chen, W.; Wong, M. W.; Andres, J. L.; Gonzalez, C.; Head-Gordon, M.; Replogle, E. S.; Pople, J. A. *Gaussian 98, Revision A.11.4*; Gaussian, Inc.: Pittsburgh, PA, 2002.

(12) (a) Vreven, T.; Morokuma, K. *J. Phys. Chem. A* **2002**, *106*, 6167–6170. (b) Vreven, T.; Morokuma, K. *J. Chem. Phys.* **1999**, *111*, 8799–8803.

(13) Curtiss, L. A.; Raghavachari, K. *Theor. Chem. Acc.* **2002**, *108*, 61–70.

(14) Möller, C.; Plesset, M. S. *Phys. Rev.* **1934**, *46*, 618–622.

(15) Lynch, B. J.; Truhlar, D. G. *J. Phys. Chem. A* **2001**, *105*, 2936–2941.

(16) Vreven, T.; Morokuma, K.; Farkas, O.; Schlegel, H. B.; Frisch, M. J. *J. Comput. Chem.* **2003**, *24*, 760–769.

(17) Energies in Table 1 are not corrected for ZPE, as they were used solely for test comparison and not as predicted values. Throughout this work, energies not corrected for ZPE are designated as raw energies and symbolized as ΔE_{DA}(raw).

(18) These enthalpies, while technically being different than ΔE_{DA} values determined computationally, have nonetheless been modeled well by various computational methods. See: Haaland, A. *Angew. Chem., Int. Ed. Engl.* **1989**, *28*, 992–1007.

(19) (a) Scott, A. P.; Radom, L. *J. Phys. Chem.* **1996**, *100*, 16502–16513. (b) Truhlar, D. G. Database of Frequency Scaling Factors for Electronic Structure Methods. http://comp.chem.umn.edu/database/freq_scale.htm (accessed July 7, 2008).

(20) (a) Diefenbach, A.; Bickelhaupt, F. M.; Frenking, G. *J. Am. Chem. Soc.* **2000**, *122*, 6449–6458. (b) Szilagyi, R.; Frenking, G. *Organometallics* **1997**, *16*, 4807–4815. (c) Ziegler, T. *Can. J. Chem.* **1995**, *73*, 743–761. (d) Ziegler, T. *Chem. Rev* **1991**, *91*, 651–667. (e) Ziegler, T. In *Metal-Ligand Interactions: from Atoms to Clusters to Surfaces*; Salahub, D. R.,Russo, N., Eds.; Kluwer: The Netherlands, 1992: pp 367−396.

(21) For examples, see: (a) Kuno, M.; Hongkrengkai, R.; Hannongbua, S. *Chem. Phys. Lett.* **2006**, *424*, 172–177. (b) Tschumper, G. S.; Morokuma, K. *J. Mol. Struct. (THEOCHEM)* **2002**, *592*, 137–147.

(22) Boys, S. F.; Bernardi, F. *Mol. Phys.* **1970**, *19*, 553–566.

(23) Chase, P. A.; Parvez, M.; Piers, W. E. *Acta Crystallogr.* **2006**, *E62*, o5181−o5183.

(24) Huheey, J. E.; Keiter, E. A.; Keiter, R. L. *Inorganic Chemistry*, 4th ed.;Harper Collins: New York, 1993; p 690.

(25) (a) Suresh, C. H. *Inorg. Chem.* **2006**, *45*, 4982–4986. (b) Boere, R. T.; Zhang, Y. *J. Organomet. Chem.* **2005**, *690*, 2651–2657.

(26) The maximum number of F. .H interactions was determined by using models to examine conformations. The values are 12 for R = Me, 18 for R = Et, and 24 for R = *i*-Pr and *t*-Bu.

(27) Timoshkin, A. Y.; Frenking, G. *Organometallics* **2008**, *27*, 371–380.

(28) (a) Welch, G. C.; Holtrichter-Roessmann, T.; Stephan, D. W. *Inorg. Chem.* **2008**, *47*, 1904–1906. (b) Finze, M.; Bernhardt, E.; Willner, H.; Lehmann, C. W. *Inorg. Chem.* **2006**, *45*, 669–678.

CT8001859